

First-principles study of shear behavior of Al, TiN, and coherent Al/TiN interfaces

S. K. Yadav,^{1,2} R. Ramprasad,² A. Misra,³ and X.-Y. Liu^{1,a)}

¹Materials Science and Technology Division, MST-8, Los Alamos National Laboratory, Los Alamos, New Mexico 87545, USA

²Chemical, Materials, and Biomolecular Engineering, Institute of Materials Science, University of Connecticut, Storrs, Connecticut 06269, USA

³Materials Physics and Applications Division, MPA-CINT, Los Alamos National Laboratory, Los Alamos, New Mexico 87545, USA

(Received 5 January 2012; accepted 10 March 2012; published online 16 April 2012)

In this *ab initio* work, density functional theory was used to calculate the ideal shear strengths of pure Al, pure TiN, the Al/TiN interfacial region, and Al/TiN multilayers. The ideal shear strength of the Al/TiN interface was found to vary from very low (on the order of the ideal shear strength of Al) to very high (on the order of the ideal shear strength of TiN), depending on whether the TiN at the interface was Ti- or N-terminated, respectively. The results suggest that the shear properties of Al/TiN depend strongly on the chemistry of the interface, Al:N versus Al:Ti terminations. Nevertheless, for the Al/TiN multilayers, the ideal shear strength was limited by shear in the Al layer away from the interface, even when the individual layer thickness is less than a nanometer.

© 2012 American Institute of Physics. [<http://dx.doi.org/10.1063/1.3703663>]

I. INTRODUCTION

The ideal shear strength—the highest achievable theoretical strength of a material—is the minimum stress needed to plastically deform an infinite dislocation-free crystal.¹ An accurate estimate of the ideal shear strength is central to understanding the limits of mechanical strength of nanostructured materials such as multilayer films, which show unusual mechanical, chemical, and electronic properties.^{2,3} Such nanoscaled multilayer films composed of metals and ceramics have been explored for their potential applications as ductile, yet strong, materials.^{4,5} It is believed that at the nanoscale, the interfaces between the two materials constituting the multilayer assume an increasingly important role in determining the properties, as they comprise a more significant volume fraction of the multilayer with decreasing layer thickness.⁶ The high strength of multilayer nanocomposites may be due to dislocations confined in a layer, which are nucleated at interfaces.

A recent experimental work on Al-TiN multilayer nanocomposites explored the effect of layer thickness of Al and TiN on hardness and flow strength.⁷ The observed high strengths were explained using the concepts of dislocation motion and interactions within the confined nanoscale Al layers. The present work attempts to test the specific role of interfaces for increased strength of multilayer nanocomposites, in the absence of dislocations. Unlike the metal-metal multilayer systems, molecular dynamics simulations to compute the interface properties are more difficult for metal-ceramic interfaces due to the lack of accurate interatomic potentials.

Using density functional theory (DFT), the ideal shear strengths of Al, TiN, Al-TiN multilayer nanocomposite, and

Al/TiN interface were calculated. The slip system of Al established by DFT results is consistent with experiments. In the case of TiN there are multiple possible slip systems as determined from the ideal shear strength calculations. The effect of interfaces on the shear behavior is explored for two geometries: (1) the Al/TiN interfacial region in a bilayer, and (2) Al/TiN multilayer with layer thickness < 1 nm.

II. METHODS

Simulations were performed using the Vienna *ab initio* simulation package (VASP),⁸ with the Perdew-Burke-Ernzerhof (PBE) generalized gradient approximation functional,⁹ and projector-augmented wave (PAW) method.¹⁰ A cut-off energy of 300 and 500 eV for the plane wave expansion of the wavefunctions was used for Al and TiN, respectively. A Monkhorst-Pack k-point mesh of at least $18 \times 18 \times 18$ and $7 \times 7 \times 7$ was required to obtain well-converged bulk modulus and lattice parameters of Al and TiN, respectively, using a primitive unit cell. Table I shows excellent agreement between the calculated and experimental values of lattice parameters, bulk modulus, and elastic constants of Al face center cubic (fcc) and TiN rock salt.

To calculate the ideal shear strength, a series of incremental shear strains were applied to the suitably chosen unit-cell. The total energy and Hellmann-Feynman stress values as a function of strain were then obtained. At each step of applied strains, a full relaxation of atomic positions was allowed. We consider two extremes of ideal shear strength. In one case, relaxation of cell shape and volume (increase in volume would be reported as percent volume increase) is allowed so that there is no stress in the system except along the shear direction. This would be referred to as pure shear. In the second case, the cell shape and volume were relaxed. Therefore, stress in directions other than the shear direction was created during the shearing process. This would be

^{a)}To whom correspondence should be addressed. E-mail: xyliu@lanl.gov.

TABLE I. Comparison of calculated and experimental values (Refs. 12 and 15) of lattice parameters, bulk modulus, and elastic constants of Al and TiN. The experimental data are room temperature data.

	Al		TiN	
	Present	Expt.	Present	Expt.
Lattice parameter (Å)	4.04	4.04	4.24	4.24
Bulk modulus (GPa)	76	79	277	288
C11 (GPa)	114	108	639	625
C12 (GPa)	61	62	139	165
C44 (GPa)	25	28	160	163

referred to as simple shear. The highest achievable shear stress in the shearing process is reported as the ideal shear strength of the material.

III. RESULTS AND DISCUSSION

A. The ideal shear strength of Al

Given that the well-established slip plane of Al is $\{111\}$, the shear strength of Al was calculated for the $\{111\}\langle 11\bar{2}\rangle$ and $\{111\}\langle 1\bar{1}0\rangle$ slip systems. Table II compares the results of the current work with available calculated values. The computed values for the simple and pure ideal shear strength of 4.2 and 3.2 GPa, respectively, for the $\{111\}\langle 11\bar{2}\rangle$ slip system of Al are in good agreement with previous DFT results.^{11,12} Both pure and simple shear strengths of Al are lower in the $\langle 11\bar{2}\rangle$ shear direction compared to the $\langle 1\bar{1}0\rangle$ shear direction. Figure 1 shows the relative movement of atoms along the $\langle 11\bar{2}\rangle$ and $\langle 1\bar{1}0\rangle$ directions. Atoms in layer 1 are fixed, and open circles show the relative movement of atoms of layer 2 during the shear process. When Al is sheared in the $\langle 11\bar{2}\rangle$ direction, the upper layer of atoms move symmetrically with respect to the lower layer, while movement of atoms due to shearing along the $\langle 1\bar{1}0\rangle$ direction is hindered. From the movement of atoms, it is intuitive that the ideal shear strength of Al is lower in the $\langle 11\bar{2}\rangle$ direction than in the $\langle 1\bar{1}0\rangle$ direction. Consistent with the relative shearing of atoms, the volume relaxation involved during pure shear is higher by 2% in the $\langle 1\bar{1}0\rangle$ direction compared to the $\langle 11\bar{2}\rangle$ direction.

B. The ideal shear strength of TiN

In an attempt to identify the slip systems of TiN, the ideal simple and pure shear strengths are calculated for

TABLE II. The simple and pure shear strength of Al for various shear systems. Values obtained in the current work are compared with the values reported in the literature (using GGA functional).

		Simple shear		Pure shear		
		Shear strength (GPa)	Shear strain	Shear strength (GPa)	Shear strain	% Volume increase
$\{111\}\langle 11\bar{2}\rangle$	Ref. 11	3.7	...	2.9
	Present	4.2	0.20	3.2	0.19	1.9
$\{111\}\langle 1\bar{1}0\rangle$	Ref. 12	3.5
	Present	6.9	0.27	4.3	0.25	4.1

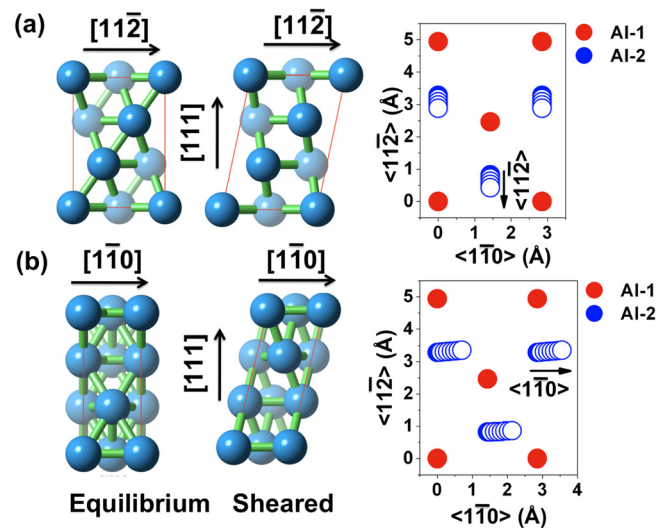


FIG. 1. First and second columns show unit cell of Al at equilibrium and sheared states, respectively. Right column shows top view (perpendicular to the shearing plane) of relative movement of atoms in layer 2 with respect to layer 1, in (a) $\langle 11\bar{2}\rangle$ direction and (b) $\langle 1\bar{1}0\rangle$ direction.

the following six shear systems: $\{111\}\langle 11\bar{2}\rangle$, $\{111\}\langle 1\bar{1}0\rangle$, $\{001\}\langle 100\rangle$, $\{001\}\langle 110\rangle$, $\{110\}\langle 1\bar{1}0\rangle$, and $\{110\}\langle 001\rangle$. Figure 2 shows the relative movement of atoms along various shear directions; layer 1 is fixed and the relative movement of atoms of layer 2 upon shearing is shown by open circles. The shear strengths of TiN in pure and simple shear states and volume relaxation corresponding to pure shear are listed in Table III.

The $\{111\}$ planes of TiN consist of alternating layers of Ti and N atoms. Ti and N atoms are symmetrically bonded to N and Ti atoms above and below, respectively. Hence, each layer moves symmetrically with respect to each other. Similar to the behavior of Al, when TiN is sheared in $\{111\}\langle 11\bar{2}\rangle$, the upper layer of atoms (N) move symmetrically with respect to the lower layer, as seen in Fig. 2(a). However, the movement of atoms due to shearing along the $\langle 1\bar{1}0\rangle$ direction is hindered by Ti atoms in the layer above and below, leading to a bending of the path of atoms along the $\langle 11\bar{2}\rangle$ direction, as shown in Fig. 2(b). Due to the symmetrical nature of atomic movements along the $\langle 11\bar{2}\rangle$ type directions, the pure shear strength of TiN is lower along $\langle 11\bar{2}\rangle$ 29 GPa as compared to the strength along $\langle 1\bar{1}0\rangle$ 35.3 GPa. Accordingly, the volume relaxation involved during pure shear is higher along $\langle 1\bar{1}0\rangle$ as compared to $\langle 11\bar{2}\rangle$.

The $\{001\}$ planes have an equal number of Ti and N atoms, with the Ti (N) atoms bonded to the N (Ti) atoms below (above). Hence, each $\{001\}$ layer is symmetrically bonded along $\langle 001\rangle$, and just two layers are sufficient to represent the relative movement of atoms. When sheared along $\langle 010\rangle$ or $\langle 110\rangle$, both Ti and N atoms move symmetrically as shown in Figs. 2(c) and 2(d). Due to the symmetric movements of atoms with no hindrance from other atoms, pure and simple shear strengths differ by a small value (of 6.7-15.7 GPa) compared to other slip planes. Also, the volume relaxations are small (1.25-1.55%) in both cases.

The $\{110\}$ planes have an equal number of Ti and N atoms in each layer, similar to the case of $\{001\}$ planes.

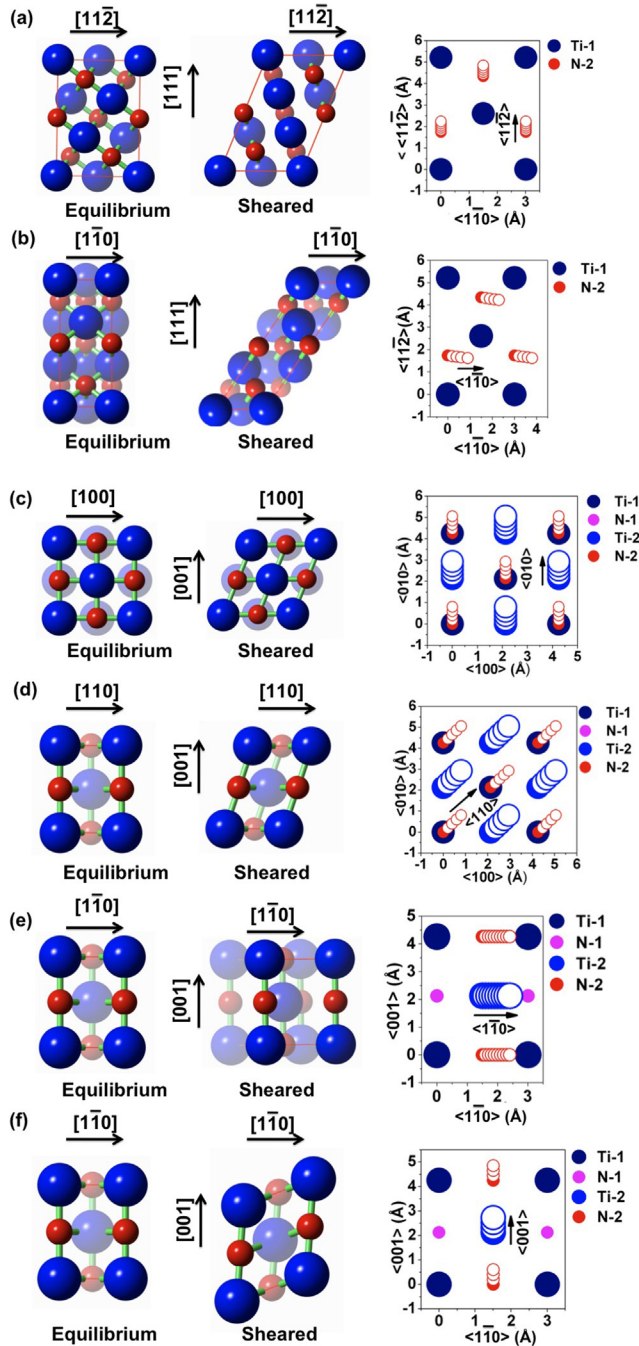


FIG. 2. First and second columns show the unit cell of TiN at equilibrium and sheared state, respectively. Right column shows the top view (perpendicular to the shear plane) of the relative movement of atoms, 1 and 2 denotes two layers involved in shearing. (a) $\{111\}\langle 11\bar{2} \rangle$, (b) $\{111\}\langle 1\bar{1}0 \rangle$, (c) $\{001\}\langle 010 \rangle$, (d) $\{001\}\langle 110 \rangle$, (e) $\{110\}\langle 1\bar{1}0 \rangle$, and (f) $\{110\}\langle 001 \rangle$.

Simple and pure shear strength of TiN in the $\{110\}\langle 1\bar{1}0 \rangle$ slip system differs by a large value (122.6 GPa), accompanied by a large volume relaxation (6.02%) in pure shear deformation. This is due to hindrance of atomic movement by the out-of-plane atoms in the adjacent layers. Pure shear strength of 29 GPa, in $\{110\}\langle 1\bar{1}0 \rangle$ shear, is in good agreement with the prior DFT calculated value of 31 GPa.¹³ For $\{110\}\langle 001 \rangle$ shear, due to symmetrical movement of atoms and no atoms to hinder, simple and pure shear strength of this shear system only differ by a small value of 9.2 GPa and the volume relaxation is as low as 1.45%.

TABLE III. The ideal shear strength of TiN for various shear systems under stress states of simple and pure shear.

	Simple shear		Pure shear		
	Shear strength (GPa)	Shear strain	Shear strength (GPa)	Shear strain	% Volume increase
$\{111\}\langle 11\bar{2} \rangle$	45.4	0.38	29.0	0.21	3.8
$\{111\}\langle 1\bar{1}0 \rangle$	121.0	0.73	35.3	0.33	10.8
$\{001\}\langle 010 \rangle$	51.2	0.42	35.5	0.28	1.6
$\{001\}\langle 110 \rangle$	39.4	0.33	32.7	0.28	1.3
$\{110\}\langle 1\bar{1}0 \rangle$	151.6	0.60	29.0[31.0 (Ref. 13)]	0.20	6.0
$\{110\}\langle 001 \rangle$	65.6	0.47	56.4	0.47	1.5

Based on the pure shear strength of TiN, we predict that there are several slip systems possible, $\{111\}\langle 11\bar{2} \rangle$, $\{111\}\langle 1\bar{1}0 \rangle$, $\{001\}\langle 010 \rangle$, $\{001\}\langle 110 \rangle$, and $\{110\}\langle 1\bar{1}0 \rangle$. All of these systems have pure shear strength close to 30 GPa. This also includes $\{111\}\langle 1\bar{1}0 \rangle$, which is the slip system of the rock salt crystal structure. As in Al, pure shear strength of TiN for $\{111\}\langle 11\bar{2} \rangle$ shear is lowest among several shear systems considered. Thus it is reasonable to assume that Al-TiN multilayer nanocomposites have the lowest ideal shear strength along the $\langle 11\bar{2} \rangle$ directions on the $\{111\}$ planes.

C. The ideal shear strength of Al-TiN multilayer

To compute the shear behavior of the Al-TiN multilayer, we consider a supercell with: (1) alternating layers of Al and TiN along the $[111]$ direction, consistent with the experimentally observed interface plane,^{7,14} (2) two layers of Al and TiN in each slab, with both layers of Al twinned with respect to each other, as observed experimentally,¹⁴ and (3) at the interface, Al atoms are in the fcc position (or site) with respect to adjacent TiN such that a fcc stacking sequence of A(Ti)B(Ti)C(Ti)A(Al) is maintained.^{7,14} For simplicity, the supercell has in-plane lattice spacings of TiN. The atomic structure of the slab for this configuration is shown in Fig. 3. We chose a minimum number of layers of Al and TiN to insure the presence of a significant interfacial effect. In all cases, the slab is sheared in the $\langle 11\bar{2} \rangle$ direction in accordance with the fact that shear strength of Al and TiN is among the lowest in $\{111\}\langle 11\bar{2} \rangle$ shear and Al/TiN interface is formed on $\{111\}$ planes.

We find that the ideal shear strength of the composite is limited by Al and is the same as the ideal shear strength of Al. Shear occurs in the twinned region for the case considered, but it can occur in the Al region or twinned Al region depending if the supercell is sheared in the $\langle 11\bar{2} \rangle$ or $\langle \bar{1}\bar{1}2 \rangle$ direction. The preference for shearing along the Al/Al layer as opposed to the Al/N interface was also noted for the case when the thickness of Al was just two atomic layers. A possible explanation for this is that the shear strength of the Al/TiN interface when the interface is N-terminated is much higher than the Al/Al layers adjacent to the interface. Thus, in multilayers with N-terminated interfaces, the interface shear may occur in the weaker Al/Al layer one atomic layer away from the interface. To further test this idea we computed the shear strength

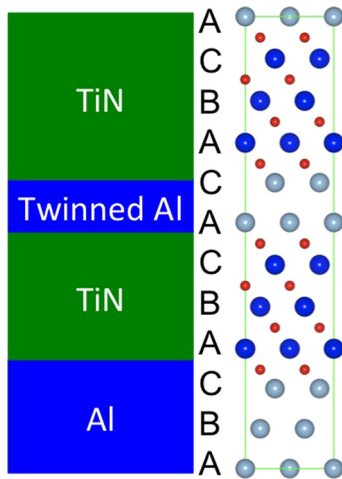


FIG. 3. Atomic structure of the Al/TiN multilayered slab used in the calculation. The TiN layer is bounded by Al layers above and below that are in twin orientation with respect to each other, consistent with experimental observation (Ref. 14). Al always sits at fcc configuration with respect to underlying TiN.

of the Al/TiN interfacial region for both N and Ti terminations, as described next.

D. The ideal shear strength of the Al/TiN interfacial region

In this section, we compute the ideal shear strength of the Al/TiN interfacial region. In the case under consideration two interface types are possible: interfacial TiN being either N- or Ti-terminated leading to, respectively, Al-N or Al-Ti bonds at the interface (referred to as the Al/N or Al/Ti interface). The shear behavior of the Al/TiN interfaces was modeled by rigidly shearing a block of Al on top of TiN along the $\langle 11\bar{2} \rangle$ directions on the $\{111\}$ plane. Supercell contains 3 layers of Al and 3 layers of TiN (3 layers of Ti and 3 layers of N), and each layer has 2 atoms. This involves shearing of Al and N or Ti bond depending on the termination.

A schematic of the interface under shear is shown in Fig. 4. The interface between materials with different lattice parameters can induce biaxial stresses. Two stress conditions were considered at the interface; Interface 1: Equal and opposite biaxial stress in Al and TiN layers at the interface; Interface 2: Al lattice parameter is stretched to match that of TiN at the interface.

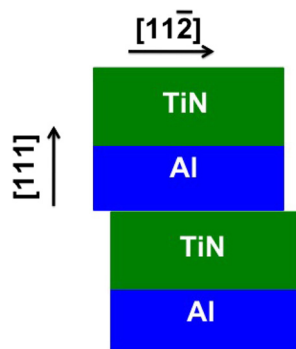


FIG. 4. Schematic representation of interface model with rigid shearing between Al and TiN at the interface.

TABLE IV. The ideal shear strength of interfaces, Al with N terminated TiN (Al/N) and Al with Ti terminated TiN (Al/Ti). Interface 1: Equal and opposite biaxial stress in Al and TiN layers. Interface 2: Al lattice parameter stretched to match TiN.

	Interface 1		Interface 2	
	Shear strength (GPa)	Shear strain	Shear strength (GPa)	Shear strain
Al/N	19.1	0.39	26.4	0.49
Al/Ti	3.3	0.18	3.2	0.18

Table IV lists the ideal shear strength of the interfaces under two types of biaxial stress states. Irrespective of the biaxial stress states at interface 1 or 2, the shear strength of the Al/Ti and Al/N interface is on the order of the ideal shear strength of Al and TiN, respectively. Moreover, the strain at the ideal shear strength is approximately equal to that in bulk Al and bulk TiN, for Al/Ti and Al/N interface, respectively. This confirms that metallic bonding exists at Al/Ti interface similar to that in Al, and covalent/ionic bonding at Al/N interface similar to that in TiN.

IV. CONCLUSIONS

In this *ab initio* work, DFT was used to study the shear behavior of pure Al, pure TiN, Al/TiN multilayer, and the Al/TiN interfacial region. For TiN, the existence of multiple slip systems is indicated by several shear systems having similarly low ideal shear strength if pure shear is considered. A key finding from this work is that the ideal shear strength of the Al/TiN interfacial region depends strongly on the interface chemistry. For N-termination, due to the strong N-Al bonding the shear strength is much higher than the case of Ti-termination with relatively weaker Ti-Al metallic bonding. Thus, the ideal shear strength of the interface is on the order of shear strengths of pure Al and pure TiN for N and Ti interfacial terminations, respectively. An implication of this finding is that in Al/TiN multilayers, if the interfaces are N-terminated the shear occurs not at the Al/N interface but at the Al/Al layer below the interface at stresses on the order of the ideal shear strength of Al. The DFT results are calculated at 0K without temperature effect into consideration. It is expected that at higher temperatures, the ideal shear stress will be reduced and from recent molecular dynamics studies of the temperature effect on ideal shear strength of Al and Cu using the embedded atom method potentials,¹⁶ the change is almost linear with increasing temperature. Further studies with dislocations at the interface are required to understand the detailed slip processes involved when the Al/TiN multilayers are plastically deformed.

ACKNOWLEDGMENTS

This work was fully supported by the U.S. Department of Energy, Office of Science, Office of Basic Sciences. The authors acknowledge discussions with Richard G. Hoagland, Jian Wang, and John P. Hirth.

- ¹A. Kelly and N. H. Macmillan, *Strong Solids*, 3rd ed. (Clarendon Press, Oxford, 1986), pp. 156.
- ²*Dekker Encyclopedia of Nanoscience and Nanotechnology*, edited by J. A. Schwarz, C. I. Contescu, and K. Putyera (CRC Press, Boca Raton, FL, 2008).
- ³M. P. Soriaga, J. Stickney, L. A. Bottomley, and Y.-G. Kim, *Thin Films: Preparation, Characterization, Applications* (Kluwer Plenum Press, NY, 2002).
- ⁴D. Bhattacharyya, N. A. Mara, R. G. Hoagland, and A. Misra, *Scr. Mater.* **58**, 874 (2008).
- ⁵G. Tang, Y.-L. Shen, D. R. P. Singh, and N. Chawla, *Acta Mater.* **58**, 2033 (2010).
- ⁶A. Misra, M. Verdier, H. Kung, J. D. Embury, and J. P. Hirth, *Scr. Mater.* **41**, 973 (1999).
- ⁷D. Bhattacharyya, N. A. Mara, P. Dickerson, R. G. Hoagland, and A. Misra, *Acta Mater.* **59**, 3804 (2011).
- ⁸G. Kresse and J. Furthmüller, *Phys. Rev. B* **54**, 11169 (1996).
- ⁹J. P. Perdew, K. Burke, and M. Ernzerhof, *Phys. Rev. Lett.* **77**, 3865 (1996).
- ¹⁰P. E. Blöchl, *Phys. Rev. B* **50**, 17953 (1994).
- ¹¹S. Ogata, J. Li, and S. Yip, *Science* **298**, 807 (2002).
- ¹²M. Jahnáček, J. Hafner, and M. Krajčí, *Phys. Rev. B* **79**, 224103 (2009).
- ¹³S.-H. Jhi, S. G. Louie, M. L. Cohen, and J. W. Morris, Jr., *Phys. Rev. Lett.* **87**, 075503 (2001).
- ¹⁴D. Bhattacharyya, X.-Y. Liu, A. Genc, H. L. Fraser, R. G. Hoagland, and A. Misra, *Appl. Phys. Lett.* **96**, 093113 (2010).
- ¹⁵M. Marlo and V. Milman, *Phys. Rev. B* **62**, 2899 (2000).
- ¹⁶A. M. Iskandarov, S. V. Dmitriev, and Y. Umeno, *Phys. Rev. B* **84**, 224118 (2011).